CYP83A1 is required for metabolic compatibility of Arabidopsis with the adapted powdery mildew fungus Erysiphe cruciferarum
C Weis, U Hildebrandt, T Hoffmann, C Hemetsberger, S Pfeilmeier, C König, W Schwab, R Eichmann, R Hückelhoven
New Phytologist 202 (4), 1310-1319, 2014
doi: 10.1111/nph.12759

https://doi.org/10.1111/nph.12759

Accepted manuscript

CYP83A1 is required for metabolic compatibility of Arabidopsis with the adapted powdery mildew fungus *Erysiphe cruciferarum*

Corina Weis[1], Ulrich Hildebrandt[2], Thomas Hoffmann[3], Christoph Hemetsberger[1], Sebastian Pfeilmeier[1], Constanze König[1], Wilfried Schwab[3], Ruth Eichmann[1] and Ralph Hückelhoven[1*]

[1]Lehrstuhl für Phytopathologie, Technische Universität München, Emil-Ramann-Straße 2, 85354 Freising, Germany;

[2]Universität Würzburg, Julius-von-Sachs-Institut für Biowissenschaften, Lehrstuhl für Botanik II , Julius-von-Sachs-Platz 3, 97082 Würzburg, Germany;

[3]Biotechnologie der Naturstoffe, Technische Universität München, Liesel-Beckmann-Str. 1, 85354 Freising, Germany

*To whom correspondence should be addressed:

E-mail: hueckelhoven@wzw.tum.de

Phone: +49 8161 71-3681

Total word count: 4.907

Word counts for each section:

Introduction: 693

Material and Methods: 867

Results: 2.019

Discussion: 1.210

Acknowledgements: 114

Number of figures: 7 /in colour: 3

Number of tables: 0

Supporting information: 5 Figures

Summary

- Aliphatic glucosinolates function in chemical defense of Capparales. The cytochrome P450 83A1 monooxygenase (CYP83A1) catalyzes the initial conversion of methionine-derived aldoximes to thiohydroximates in the biosynthesis of glucosinolates and thus *cyp83a1* mutants have reduced levels of aliphatic glucosinolates.
- Loss of CYP83A1 function leads to dramatically reduced parasitic growth of the biotrophic powdery mildew fungus *Erysiphe cruciferarum* on *Arabidopsis thaliana*. The *cyp83a1* mutants support less well the germination and appressorium formation of *E. cruciferarum* on the leaf surface and post penetration conidiophore formation by the fungus. By contrast, a *myb28-1 myb29-1* double mutant, which totally lacks aliphatic glucosinolates, shows wild type level of susceptibility to *E. cruciferarum*.
- The *cyp83a1* mutants also lack very-long-chain aldehydes on their leaf surface. Such aldehydes support appressorium formation by *E. cruciferarum in vitro*. Additionally, when chemically complemented with the C26 aldehyde *n*-hexacosanal, *cyp83a1* mutants could again support appressorium formation. The mutants further accumulate 5-methylthiopentanaldoxime, the potentially toxic substrate of CYP83A1.
- Loss of powdery mildew susceptibility by *cyp83a1* may be explained by a reduced supply of the fungus with inductive signals from the host and an accumulation of potentially fungitoxic metabolites.

Key words: aldoximes, aliphatic glucosinolates, BAX INHIBITOR-1, cytochrome P450 monooxygenase, metabolon, powdery mildew, susceptibility, very-long-chain aldehydes

Introduction

Compatibility of plants and microbial pathogens leads to disease and symptom development. However, compatibility is rare in nature whereas resistance or incompatibility is common. This is explained by several aspects of host-parasite interactions. Compatibility requires the adaptation of a pathogenic microbe to its host (Morrissey & Osbourn 1999; Thordal-Christensen, 2003). An adapted pathogen can recognize specific host-derived signals that trigger pathogen differentiation and expression of virulence or both. Therefore, pathogens have to adapt to the chemical composition of their hosts. This leads to the evolution of an enzymatic toolbox, which the pathogen uses to overcome structural and chemical barriers of their hosts or to metabolize host-derived substrates. In addition, plants possess robust innate immunity that involves defense responses triggered after recognition of pathogen-derived elicitors (microbe-associated molecular patterns or pathogen effectors) or of host-derived elicitors (damage-associated molecular patterns) (Maekawa *et al.,* 2011; Boller and Felix, 2009). Consequently, pathogens require host-specific effector molecules that match host targets for suppression of immunity and reprogramming the host for the demands of the pathogen. Loss of susceptibility, therefore, may result from altered host immunity (gain of resistance functions) or, in a more strict sense, from changes in host components that are required by the microbe for pathogenesis but do not directly operate in regulation of defense (de Almeida Engler et al. 2005; Hückelhoven et al. 2005; Pavan et al. 2010; Hückelhoven et al. 2013).

In contrast to wild type Arabidopsis plants, loss of function mutants of the cytochrome P450 monooxygenase CYP83A1 gene are barely susceptible to the biotrophic ascomycete *Erysiphe cruciferarum* (Weis *et al.,* 2013), which causes powdery mildew on many Brassicaceae (Adam *et al.,* 1999). The cytochrome P450 gene family in *Arabidopsis* comprises 244 genes (and 28 pseudogenes) and constitutes one of the largest gene families in plants. P450 enzymes function as monooxogenases in the biosynthesis of diverse metabolites, including pigments, phytohormones, lignin, or defense compounds such as flavonoids, alkaloids, or glucosinolates

(reviewed in Bak *et al*., 2011). The synthesis of aliphatic glucosinolates is divided into three stages, the chain elongation of the amino acid, formation of the glucosinolate core structure, and finally secondary modifications (Wittstock & Halkier, 2002). The two CYP83 proteins CYP83A1 and CYP83B1, phylogenetically belong to the CYP71 clade (Hansen *et al*., 2001; Bak *et al*., 2011). They non-redundantly function in the core structure synthesis of glucosinolates by catalyzing the initial conversion of aldoximes to thiohydroximates (Bak & Feyereisen, 2001; Naur *et al*., 2003). CYP83A1 has higher substrate specificity for methionine-derived aldoximes in the synthesis of aliphatic glucosinolates whereas CYP83B1 preferentially converts tryptophan-derived aldoximes in the synthesis of indole-glucosinolates (Bak & Feyereisen 2001, Naur *et al.,* 2003).

In plant-herbivore interactions, glucosinolates and their hydrolysis products such as isothiocyanate, nitrils, or epithionitrils, function as deterrents against generalist herbivores but also as attractants for specialized insects. The knowledge about the function of glucosinolates in plant-fungus interaction is more limited (Bednarek and Osbourn, 2009). However, in *Arabidopsis*, the peroxisome-associated myrosinase PENETRATION 2 (PEN2) hydrolyses 4-methoxyindol-3-ylmethylglucosinolate to bioactive products involved in resistance to non-adapted powdery mildew fungi (Lipka *et al.,*2005, Bednarek *et al.,*2009). Indole-glucosinolates are further important to balance the mutualistic interaction of *Arabidopsis* with the beneficial root endophyte *Piriformospora indica* (Jacobs et al. 2011; Nongbri *et al*., 2012). Aliphatic glucosinolates are important in resistance to lepidopteran larvae, to non-adapted bacterial pathogens, and to the necrotrophic fungus *Sclerotinia sclorotiorum* (Beekwilder *et al*., 2008; Fan *et al.*, 2011; Stotz *et al.*, 2011). However, little information is available about the role of aliphatic glucosinolates in interaction with haustorium-forming fungi.

Powdery mildew fungi are obligate biotrophic ascomycete pathogens with a high degree of specialization to a limited range of hosts. They form haustoria from appressoria that sense and directly penetrate the host cuticle and cell wall (Green *et al.,* 2002; Hückelhoven & Panstruga,

2011). *E. cruciferarum* is a typical powdery mildew fungus adapted to Brassicaceae (Adam *et al*., 1999). Hence, it can normally cope with glucosinolates due to unknown mechanisms.

In this study, we report about a so far uncharacterized function of CYP83A1 in interactions with fungal pathogens. Loss of *CYP83A1* changes the metabolic composition of *Arabidopsis* in a way that greatly influences the interaction outcome with biotrophic and necrotrophic ascomycetes.

Material and Methods

Plants, pathogens and inoculation

Arabidopsis thaliana ecotype Col-0 was purchased from Lehle Seeds (Round Rock, USA). *cyp83a1-1* (Weis *et al.,* 2013), *cyp83a1-2* (= *ref2-1*; Hemm *et al*., 2003), and *myb28-1 myb29-1* (Sønderby *et al*., 2007) were described before. *Arabidopsis* seeds were sown in a soil sand mixture and stratified for 2 days at 4°C before placement in a growth chamber at 22°C, a photoperiod of 10 h, and 64% relative humidity.

E. cruciferarum was maintained on Col-0, and on super-susceptible phytoalexin-deficient *pad4* mutants (Reuber *et al*., 1998). Plants and glass slides were inoculated with a density of 3-5 and 10-15 *E. cruciferarum* conidia per mm^2, respectively, as described previously (Weis *et al*., 2013).

Botrytis cinerea strain B05.10 was cultivated on Gamborg's B5 plates (Duchefa Biochemie BV) containing 2% glucose. Based on a protocol of Gronover *et al.* (2001), conidia were washed-off of 7-10-day-old plates, and adjusted to a final concentration of 2 x 10^5 conidia per ml using Gamborg's B5 medium containing 2% glucose and 10 mM KH_2PO_4 (pH 6.4). Upon pre-germination for 1 h at RT, 20 µl of the suspension were dropped on leaves of about 5-week-old *Arabidopsis* plants. Plants were further cultivated covered with a plastic cap under normal growth conditions. *B. cinerea* symptoms were evaluated 3 days after inoculation (dai) by calculating the affected leaf area.

Staining methods

Acetic ink staining of epiphytically grown structures of *E. cruciferarum* was performed as previously described (Weis *et al.,* 2013). Wheat germ agglutinin-tetramethylrhodamin (WGA-TMR, Invitrogen Molecular Probes GmbH Karlsruhe, Germany) was used to stain fungal structures including haustoria. Discolored leaves were vacuum infiltrated with a staining solution, containing 10 µg WGA-TMR and 10 µg BSA per ml PBS, and were incubated over

night in the staining solution at 4°C. Samples were observed via fluorescence-microscopy (Leica DM 1000). Callose staining of WGA-TMR treated leaves was performed by using 0.05% (w/v) methyl blue in 0.067 M potassium phosphate buffer (pH 5.8). Vacuum was applied twice and leaves were stored in the staining solution over night at 4°C.

In order to assess cuticle permeability, Calcofluor white staining of leaves of about 5-week old plants was performed as described by Bessire *et al.* (2007). The incubation time was set to 30 sec. Calcofluor white was detected under a Zeiss Axioimager Z1 (Zeiss, Jena, Germany) fluorescence microscope using a 368 nm excitation filter, a 385 nm dichromatic mirror, and a 420 nm suppression filter.

Chlorophyll leaching

7-week-old single rosette leaves were collected and immersed each in 6 ml 80% ethanol in plastic tubes and then gently agitated on a shaker platform in darkness at 25°C. The amount of chlorophyll extracted into the solution was quantified using a UV4-500 UV/VIS spectrophotometer (UNICAM) and calculated from light absorption at 647 and 664 nm as described by Lolle *et al*. (1997). For that purpose 1 ml aliquots were measured every 20 min after initial immersion over a 2 h period. Each aliquot was poured back into the same tube after measurement. Data are given as µmoles chlorophyll per cm^2 leaf surface area.

Cuticular wax analysis

Leaf cuticular waxes were extracted by immersing 30 intact, 7-week-old *Arabidopsis* rosette leaves for 1 min in 10 ml chloroform at room temperature. The solvent was evaporated under a gentle flow of nitrogen. Sample derivatization, GC/MS and GC/FID analyses were performed as described previously (Hansjakob *et al*., 2010). Five replicate samples per plant line were analysed. Statistical analysis was carried out using the Mann–Whitney-U-test for every wax component.

Coating of glass slides and plants

Glass slides were coated with 0.5% Formvar® resin together with the C_{26} alkane *n*-hexacosane to a final concentration of 6.8 x 10^{-4} mol l^{-1}, or additionally with the C_{26} aldehyde *n*-hexacosanal or the C_{30} aldehyde *n*-triacontanal to a final concentration of 6.8 x 10^{-5} mol l^{-1} in the dipping solution as previously described by Hansjakob *et al.* (2010). Depending on the molecular weight of the molecule, a concentration of 6.8 x 10^{-5} mol l^{-1} of *n*-hexacosanal or *n*-triacontanal in the dipping solution corresponds to a glass surface coverage of c. 50–60 ng cm^{-2}, which roughly reflects the amount of very-long-chain aldehydes present per cm^2 Arabidopsis leaf surface area.

For chemical applications, detached leaves were placed on water agar and sprayed by the use of a chromatography sprayer with solutions of n-hexacosane or n-hecacosanal in chloroform (each 5mg mL^{-1}). Mock-treated plants were sprayed with pure chloroform. After evaporation of the solvent, leaves were inoculated with fungal conidia at a density of 4 conidia mm^{-2}. At some points, bigger droplets of chloroform caused small necrotic lesions on the leaves. These areas were excluded from microscopic evaluation. At 8 h after inoculation, leaves were fixed and stained for microscopy of fungal infection structures (see above).

Analytical LC-MS

50 mg frozen plant material was extracted with 2 ml methanol. Methanol was removed in a Speed-Vac concentrator and the extract was re-dissolved in 100 µl methanol for analysis by liquid chromatography/electrospray ionization multistage mass spectrometry (LC-ESI-MS^n) according to Yin *et al.* (2012). Data analysis was performed using the DataAnalysis 3.1 software (Bruker Daltonics). Untargeted metabolite profiling was performed using XCMS (Smith *et al*., 2006). Synthetic 5-methylthiopentanaldoxime (Dawson et al. 1993) served as an external standard.

Results

Germination and penetration processes of *E. cruciferarum* are delayed on *cyp83a1* mutants

Recently, we reported on a strong loss of susceptibility to the powdery mildew fungus *E. cruciferarum* for two independent *cyp83a1* mutants (Weis *et al.,* 2013). However, the mechanistic basis of this phenotype was unclear. We therefore investigated the early development of *E. cruciferarum* on the leaf surface of *cyp83a1* mutants (Fig. 1 a,b). Col-0, *cyp83a1-1*, and *cyp83a1-2* plants were inoculated with conidia of the adapted powdery mildew fungus *E. cruciferarum* and analyzed 3 and 8 h after inoculation (hai). The developmental stage of the conidia was divided in non-germinated conidia, conidia showing appressorial germ tubes (AGT) without a mature appressorium, or formation of a mature lobed appressorium (APP) (Fig. 1c). We observed a significantly enhanced percentage of non-germinated conidia on *cyp83a1-1* and *cyp83a1-2* when compared to Col-0 at 3 hai. Consistent with this, the percentage of conidia with developing AGT was strongly reduced on both mutants. Only very few conidia had formed an APP at 3 hai. By 8 hai, the majority of conidia had formed an APP on Col-0, (53%) whereas much less conidia had already developed an APP on *cyp83a1-1* (22%) and *cyp83a1-2* (37%) (Fig. 1a).

Additional microscopic analyses were carried out 2 d after inoculation (dai). In this case, only germinated conidia were analyzed in respect of APP formation without penetration (APP), establishment of a first haustorium (HAU) with formation of elongated hyphae (EH), or the subsequent formation of secondary haustoria (sec HAU) (Fig. 1d). On the wild type, about 14% of the conidia were in a stage, where the appressorium (APP) had been formed without successful haustorium formation. However, the majority of fungi (71%) had established a haustorium and elongated hyphae (EH) by this time. 15% of the fungi already established a secondary haustorium in the host cells. By contrast, the number of conidia with an APP only, was significantly enhanced on *cyp83a1-1* and *cyp83a1-2* to 45% and 40%, respectively.

Consequently, the number of fungi with haustoria and elongated hyphae was significantly reduced to 53% on *cyp83a1-1* and to 59% on *cyp83a1-2*. The percentage of conidia, which established secondary haustoria was also significantly reduced on both *cyp83a1* mutants. On *cyp83a1-1* and *cyp83a1-2* only 1% of the germinated *E. cruciferarum* conidia had established secondary haustoria, respectively (Fig. 1b).

Finally, we evaluated local and whole cell callose deposition as typical plant responses to powdery mildew fungi (Micali *et al*., 2008, and Fig. 1e). No significant differences in local callose deposition were detected in both *cyp83a1* mutants when compared to the wild type at 2 dai. In Col-0, *cyp83a1-1*, and *cyp83a1-2,* callose deposition was visible in about 90% of the attacked or penetrated epidermal cells (Fig. 1f). Whole-cell-callose accumulation, indicative of cell death (Jacobs et *al*., 2003), was rare at 2dai. The percentage of interaction sites with cell death was slightly enhanced on *cyp83a1-1* and *cyp83a1-2*, compared to the wild type (Fig. 1f) but this could not explain the strong resistance phenotype of the mutants.

In summary, data indicate that that germination and penetration of *E. cruciferarum* are substantially delayed on both *cyp83a1* mutants when compared to the wild type Col-0. However, the mutant's cellular defense of the fungus appears only marginally altered.

Aliphatic glucosinolates are not required for the development of *E. cruciferarum*

The T-DNA knock-out mutant *cyp83a1-1* and the loss of function point mutant *cyp83a1-2* (= *ref2-1, reduced epidermal fluorescence2-1*) have a strongly reduced content of aliphatic glucosinolates when compared to the wild type Col-0 (Hemm *et al.,* 2003; Weis *et al.,* 2013). Because chemical defense might alternatively serve as signal for fungal development when overcome by adapted parasites, we tested whether *E. cruciferarum* normally infects the *myb28-1 myb29-1* double mutant, which lacks aliphatic glucosinolates (Sønderby *et al*., 2007). 5-week old Col-0, *cyp83a1-1*, *cyp83a1-2*, and *myb28-1 myb29-1* plants were inoculated with conidia of *E. cruciferarum*. As previously shown, both *cyp83a1* mutants were

only little susceptible to powdery mildew compared to Col-0 (Fig. 2a, Weis *et al*., 2013). Microscopy confirmed this observation by evaluation of the number of conidiophores per fungal colony 5 dai (Fig. 2b). However, the *myb28-1 myb29-1* double mutant showed wild type-like *E. cruciferarum* colonization both macroscopically and microscopically (Fig. 2). Hence, aliphatic glucosinolates appear to be not required for a compatible interaction of *Arabidopsis* with *E. cruciferarum*.

Since previous results suggested that *cyp83a1* mutants are affected in their ability to contain cell death after treatment with a fungal toxin (Weis *et al.,* 2013), we tested whether CYP83A1 had an impact in the interaction of *Arabidopsis* with a necrotrophic pathogen. Therefore we inoculated Col-0, *cyp83a1-1*, *cyp83a1-2*, and *myb28-1 myb29-1* plants with the necrotrophic fungus *Botrytis cinerea*. Interestingly, a strongly pronounced symptom development was observed on the *myb28-1 myb29-1* mutant (Supporting Information Fig. S1). Both *cyp83a1* mutants also showed significantly increased susceptibility to necrotization by *B. cinerea* when compared to the wild type Col-0 at 3 dai. However, they were less susceptible to *B. cinerea* than the *myb28-1 myb29-1* mutant (Supporting Information Fig. S1). This suggested a function of aliphatic glucosinolate metabolism in basal resistance to *B. cinerea.*

cyp83a1 mutants exhibit an altered leaf cuticular wax composition

In the course of the microscopic analysis of the powdery mildew phenotype, we observed a cuticle/wax phenotype on both *cyp83a1* mutants. On *cyp83a1* mutants, acetic ink not only visualized epiphytically grown fungal structures but also haustoria and chloroplasts, which were not reached by the dye on wild type samples (not shown). To confirm increased cuticle permeability, Calcofluor white staining was conducted as previously described by Bessire *et al*. (2007). Fluorescence of Calcofluor white occurs after binding to cellulose and thus indicates penetration of the dye through the cuticle of plants. We observed a strong laminar Calcofluor white fluorescence of *cyp83a1-1* and *cyp83a1-2* leaves but not of Col-0, where

only marginal fluorescence was detected (Fig. 3a). Leaves of *myb28-1 myb29-1* showed wild type-like Calcofluor fluorescence (Supporting Information Fig. S2). A chlorophyll leaching assay showed faster chlorophyll release from leaves of *cyp83a1-1* and *cyp83a1-2* than from leaves of Col-0 (Fig. 3b). Together this suggested an altered cuticle/wax composition of the *cyp83a1* mutants.

To further investigate the cuticular wax composition of *cyp83a1* mutants, the leaf surface of *Arabidopsis* leaves was extracted with chloroform and subjected to GC-FID/GC-MS analysis. This revealed a significantly reduced amount of total wax in *cyp83a1-1* and *cyp83a1-2* compared to Col-0 (Supporting Information Fig. S3a). Moreover, the composition was changed of the major single substance classes of the *Arabidopsis* leaf cuticular wax, alkanoic acids (fatty acids), *n*-alkanes, primary alkanols, branched alkanols, *n*-aldehydes, and sterols. The data indicate significant differences in the content of branched alkanols and aldehydes in the wax layer of Col-0 compared to both *cyp83a1* mutants (Supporting Information Figure S3). The percentage of branched alkanols was slightly enhanced in *cyp83a1-1* and *cyp83a1-2* whereas the amount of aldehydes was dramatically reduced in both mutants when compared to the wild type Col-0. In fact, no aldehydes were detectable in the leaf cuticular wax of *cyp83a1-1* or *cyp83a1-2* (Fig. 4).

Furthermore, we measured significant differences in respect to the chain length of the components. For instance, an obvious shift from C_{32} - C_{36} fatty acids to C_{24} - C_{28} fatty acids in both *cyp83a1* mutants was detected (Supporting Information Fig. S3c). The amount of *n*-alkanols, in particular of C_{28}, C_{29}, and C_{30} *n*-alkanols, was significantly enhanced in *cyp83a1-1* and *cyp83a1-2*, respectively, when compared to Col-0 (Supporting Information Fig. S3d). No obvious differences in *n*-alkane composition were observed (Supporting Information Fig. S3e). In summary, significant differences were observed in the amount and in the composition of the leaf cuticular wax in *cyp83a1-1* and *cyp83a1-2* compared to the wild type. Most

remarkable, very-long-chain aldehydes were absent from the wax layer of both *cyp83a1* mutants.

Very-long-chain aldehydes promote appressoria formation by *E. cruciferarum*

The cuticular wax composition is a crucial factor for germination of fungal conidia and subsequent penetration of host barriers (Podila et al., 1993; Kolattukudy *et al*., 1995; Tsuba *et al*., 2002; Zabka *et al*., 2008, Inada & Savory, 2011; Hansjakob *et al*., 2010, 2012). Very-long-chain aldehydes were shown to function as signals to initiate germination and appressorium differentiation of the powdery mildew fungus *Blumeria graminis* f.sp. *hordei* on its host barley (Tsuba *et al*., 2002; Zabka *et al*., 2008; Hansjakob *et al*., 2010, 2012). Since *cyp83a1* mutants lacked very-long-chain aldehydes, we tested whether such aldehydes can trigger germination and differentiation of *E. cruciferarum*. Therefore, we coated glass slides with Formvar®-resin and the C_{26} alkane *n*-hexacosane, or additionally with the C_{26} aldehyde *n*-hexacosanal or the C_{30} aldehyde *n*-triacontanal and inoculated them with conidia of *E. cruciferarum.* We microscopically analyzed fungal development by 9 hai. The developmental stage of the conidia was divided in non-germinated conidia, conidia showing an immature appressorial germ tube (AGT) or a mature appressorium (APP) (Fig. 5b). On *n*-hexacosane-coated slides, the majority of conidia of *E. cruciferarum* (77%) did not germinate. 17% of the conidia formed an appressorial germ tube (AGT), and only 6% established a mature appressorium (APP). In contrast, on *n*-hexacosanal- and *n*-triacontanal-coated glass slides the percentage of non-germinated conidia was significantly reduced to 44% and 54%, respectively. The percentage of conidia, which formed only an AGT was also reduced to 9% on *n*-hexacosanal-containing slides and significantly reduced to 7% on *n*-triacontanal-coated slides. Simultaneously, the amount of conidia showing mature APP formation significantly increased to 47% and to 40% on glass slides coated with the C_{26} and C_{30} aldehydes, respectively (Fig. 5a). To further test whether the lack of very-long-chain aldehydes might be

responsible for the delay in fungal development on *cyp83a1* mutants, we performed a chemical complementation experiment. Therefore, we sprayed detached leaves of wild type and *cyp83a1-2* with the aldehyde *n*-hexacosanal solved in chloroform, the corresponding alkane *n*-hexacosane or mock-treated them with chloroform alone. At 8 hours after inoculation, the fungus had developed mature APP from about 70% of the conidia in the wild type control, but only from about 35% of conidia on *cyp83a1-2*. The alkan *n*-hexacosane did not promote germination or APP formation on *cyp83a1-2*. By contrast, *n*-hexacosanal complemented the rate of germination and APP formation on *cyp83a1-2* to the level of the wild type control but did not further promote fungal development on the wild type (Fig. 6). In summary, very-long chain aldehydes promote germination and differentiation processes of *E. cruciferarum* conidia *in vitro* and on plants.

Accumulation of unidentified metabolites and 5-methylthiopentanaldoxime in *cyp83a1* mutants

To further chemically phenotype the mutants, we conducted analytical LC-MS of methanol-extracts from leaves. LC-MS-based metabolomic data were analyzed using XCMS (Smith *et al*., 2006) to identify differences in the metabolic profiles of Col-0, *cyp83a1-1*, *cyp83a1-2*, and *myb28-1 myb29-1*. According to this, mutations in *CYP83A1* had a severe and statistically significant effect on the content of many soluble metabolites as described before for phenylpropanoids for *cyp83a1-2*/*ref2-1* (Hemm *et al.*, 2003). Most of the differentially accumulating metabolites were specifically enriched or depleted in *cyp83a1* mutants (Supporting Information Fig. S4).

Since CYP83A1 catalyzes the initial conversion of methionine-derived aldoximes to S-alkyl-thiohydroximate, we wondered whether aldoximes might accumulate in *cyp83a1* mutants as suggested earlier by Hemm and associates (2003). Since oximes are toxic to fungi (Møller, 2010), an accumulation of methionine-derived aldoximes might further contribute to

resistance of the *cyp83a1* mutants to *E. cruciferarum*. Hence, we conducted analytical LC-MS measurements using 5-methylthiopentanaldoxime (5-MTPO) as external standard. 5-MTPO is the precursor of the major aliphatic glucosinolates, e.g. 4-methylsulphinylbutylglucosinolate, in *Arabidopsis* Columbia-0 leaves (Haughn *et al*., 1991; Hansen *et al*., 2001). Methanol-extracts of *cyp83a1-1* and *cyp83a1-2* leaves showed a peak of the ion trace at m z^{-1} 148, identical in retention time and fragmentation pattern to the standard 5-MTPO (Fig. 7a, Supporting Information Fig. S5). Another even more pronounced peak was detected in both independent *cyp83a1* mutants with the same m z^{-1} and fragmentation pattern as 5-MTPO but different retention time. This peak likely represents an isomer of 5-MTPO (Fig. 7b, Supporting Information Fig. S5). In samples of either Col-0 or *myb28-1 myb29-1*, peaks of the 5-MTPO and 5-MTPO isomer were negligible (Fig. 7).

Together, we detected strong metabolic perturbation and a specific accumulation of 5-MTPO, the substrate of CYP83A1, in *cyp83a1* mutants when compared to Col-0.

Discussion

Loss of disease susceptibility occurs in mutants with constitutive or primed defense responses. Other mutants do not support pathogenesis because they lack components on which the pathogen relies for accommodation of infection structures (Hückelhoven et al. 2013). Alternatively, mutants can lose susceptibility because of changes in their chemical composition. This may involve lack of nutrients or cues for proper development of the pathogen, or accumulation of antibiotic substances. The *cyp83a1/ref2* mutants analyzed here may represent an example with altered host chemical composition. Mutants actually show both lack of cuticular wax components that *E. cruciferarum* obviously recognizes for appressorium differentiation as well as an accumulation of a potentially fungitoxic aldomixe.

Metabolic changes in *cyp83a1* mutants cause chemical incompatibility with *E. cruciferarum*

Loss of function mutations of *cyp83a1* cause metabolic perturbation in *Arabidopsis* (Hemm et al. 2003). In accordance with this, we measured strong differences in concentration of many methanol-soluble metabolites (see also Supporting Information Fig. S4). Specific phenotypes in the host-parasite interaction support the view that certain metabolic changes may largely explain altered development of *E. cruciferarum* on *cyp83a1*. *E. cruciferarum* showed delayed germination and differentiation of appressoria on the leaf surface of *cyp83a1* mutants and developed dramatically less conidiophores per microcolony post penetration. This supported the view that fungal development was hampered on *cyp83a1* both during initiation and maintenance of pathogenesis. It appears possible that distinct metabolic changes are responsible for failure of *E. cruciferarum* to develop on cyp83a1 before and after penetration of the host cuticle.

Adapted pathogens may utilize chemical defense compounds of their host as cues or nutrients for their own development (e.g. Nielsen et al. 2006). We therefore speculated that reduced amounts of aliphatic glucosinolates might cause loss of susceptibility to the adapted powdery mildew fungus *E. cruciferarum*. However, the *myb28-1 myb29-1*double mutant, which does not contain significant amounts of aliphatic glucosinolates (Sønderby *et al.,* 2007; Beekwilder *et al.,* 2008; Sønderby *et al.,* 2010), displayed wild type-like susceptibility to *E. cruciferarum.* Therefore, reduced amounts of aliphatic glucosinolates *per se* do not explain why *cyp83a1* mutants do not support powdery mildew. Recently, it was also reported that the *myb28 myb29* double mutant shows unaltered susceptibility to *Phytophthora capsici,* too (Wang *et al.,* 2013). Interestingly, both the *myb28-1 myb29-1* double mutant and *cyp83a1* mutants were extremely susceptible to the grey mold fungus *B. cinerea*, which belongs to the Leotiomycetes class of the Ascomycota like *E. cruciferarum* (compare Fig. 2, Supporting information Fig. S1). Therefore, data suggest that an intact aliphatic glucosinolate metabolism is required for

basal resistance to *B. cinerea*, whereas *E. cruciferarum* can cope with basal levels of aliphatic glucosinolates in the wild type.

Aldoximes are highly reactive and potentially cytotoxic (Drumm *et al.,* 1995; Sakurada *et al*., 2009). It was suggested that wild type plants channel precursors and intermediates of the glucosinolate metabolism through multienzyme complexes, so-called metabolons, which allow for controlled release of products. Metabolons may be required to prevent undesired release of reactive metabolites that can interfere with other metabolic pathways (Møller, 2010). The characterization of *ref2* mutants, which are defective in *CYP83A1* (Hemm *et al.*, 2003), provided indirect support for the existence of a glucosinolate metabolon. *cyp83a1/ref2* mutants show defects in phenylpropanoid metabolism, and it was suggested that aldoximes, which are processed by CYP83A1 in the wild type, accumulate in *cyp83a1/ref2* mutants and inhibit enzymes of the phenylpropanoid metabolism such as caffeic acid O-methyltransferase. As a result, sinapoyl malate as an O-methylated product of phenylpropanoid metabolism is absent from the *ref2* mutants, explaining lack of epidermal fluorescence (Hemm *et al.*, 2003). Here, we show that *cyp83a1/ref2* mutants indeed accumulate the postulated CYP83A1 substrate aldoxime 5-MTPO. Aldomixes are toxic to fungi and considered as potential antibiotics and biofungicides (Drumm *et al.,* 1995). Together, it seems possible that aldoximes contribute to inhibition of post-penetration growth of *E. cruciferarum* on *cyp83a1*.

We originally discovered CYP83A1 in a biochemical screening for interaction partners of BAX INHIBITOR-1 (BI-1) (Weis *et al.,* 2013). BI-1 is an endoplasmic reticulum (ER)-resident protein that controls cell death and susceptibility to biotic and abiotic stress. BI-1 further modulates plant metabolism and is a direct interactor of cytochrome b5 in fatty acid hydroxylation (Ishikawa *et al.,* 2013). We do not yet understand the function of the molecular interaction of BI-1 and CYP83A1. However, it is tempting to speculate that BI-1 could function in the assembly or stabilization of ER-resident metabolons, perhaps as a molecular

scaffold. BI-1 could thus support coordinated metabolism under stress conditions and protect the plant from uncontrolled release of cytotoxic metabolites.

Lack of very-long-chain fatty aldehydes in *cyp83a1* mutants explains developmental defects of *E. cruciferarum*

The initial observation that acetic ink can penetrate the cuticle/wax layer of fixed leaves of *cyp83a1* provoked a more detailed analysis. This suggested that the physicochemical properties of the cuticle of *cyp83a1* mutants were altered. The mutants showed a greatly enhanced permeability for soluble substances into and out of leaves (Fig. 3). Accordingly, our analytical data showed an altered amount and composition of *cyp83a1* wax when compared to wild type. Most strikingly, very-long-chain aldehydes were absent from the chloroform extracts whereas very-long-chain alcohols were increased and very-long-chain fatty acids were increased or decreased depending on the chain length. Data suggest a so far unrecognized metabolic phenotype of *cyp83a1* mutants in the biosynthesis of very-long-chain fatty substances. It needs to be elucidated whether CYP83A1 itself could be directly involved in fatty acid metabolism such as other cytochrome p450 monooxygenases (Höfer *et al*., 2008; Pinot & Beisson, 2011).

Exemplary very-long-chain aldehydes were able to promote conidia germination and appressorium differentiation of *E. cruciferarum* in *vitro.* This is in accordance with the finding that very-long-chain aldehydes promote differentiation of other powdery mildew fungi, too (Tsuba *et al*., 2002; Zabka *et al*., 2008; Hansjakob *et al*., 2010, 2012). Importantly, the very-long-chain aldehydes were sufficient to chemically complement *cyp83a1* mutants in terms of fungal germination and support of appressorium formation. This suggests that a lack of very-long-chain aldehydes on the surface of *cyp83a1* mutants fully explains delayed differentiation of fungal infection structures. Chemical complementation of early fungal development suggests a pivotal function of the very-long-chain aldehydes in chemical

compatibility, which appears to be conserved in monocots and dicots. *E. cruciferarum* many times penetrates the cuticle and cell wall of wild type Arabidopsis for formation of haustoria before it sporulates. It is therefore possible that the lack of sporulation can be also partially explained by a cumulative effect from multiple failed or delayed penetration events. This might be supported by the fact that *E. cruciferarum,* once it had germinated, was also delayed in formation of second haustoria (Fig. 1b).

Together, *E. cruciferarum* is well adapted to the chemical composition of *Arabidopsis thaliana*. It utilizes very-long chain aldehydes at the plant surface as chemical cues for induction and differentiation of infection structures and can cope with aliphatic glucosinolates in the wild type. Genetic disruption of aliphatic glucosinolate metabolism interfered with this chemical compatibility with this powdery mildew fungus at CYP83A1 but not at the level of pathway regulation level by MYB28 and MYB29. We suggest that very-long chain aldehydes are pivotal for chemical compatibility at the level of fungal penetration. Failure of fungal sporulation might be explained by a cumulating effect of multiple penetration failures and potential fungitoxic metabolites that accumulate in *cyp83a1* mutants.

Acknowledgements

We thank Katharina Beckenbauer, Andrea Knorz and Johanna Hofer for excellent technical support. We are grateful to Barbara Halkier and Meike Burow (University of Copenhagen, Denmark) for providing the *myb28-1 myb29-1* mutant, and to Clint Chapple (Purdue University, West Lafayette, USA) for providing the *ref2* mutant. The standard 5-methylthiopentanaldoxime was generated in the lab of John Pickett (Rothamsted Research, Harpenden, UK) and obtained from Barbara Halkier. The *Botrytis cinerea* strain B05.10 was kindly provided by Paul Tudzynski (Westfälische-Wilhelms-Universität, Münster, Germany). Financial support for the project came from grants from the German research foundation to

R.E. and R.H. (DFG EI835/1) and to the labs of R.H. and W.S. in the collaborative research centre SFB 924.

References

Adam L, Ellwood S, Wilson I, Saenz G, Xiao S, Oliver RP, Turner JG, Somerville S. 1999. Comparison of *Erysiphe cichoracearum* and *E. cruciferarum* and a survey of 360 Arabidopsis thaliana accessions for resistance to these two powdery mildew pathogens. *Molecular Plant-Microbe Interactions* **12**: 1031-1343.

Bak S, Feyereisen R. 2001. The involvement of two p450 enzymes, CYP83B1 and CYP83A1, in auxin homeostasis and glucosinolate biosynthesis. *Plant Physiology* **127**: 108-18.

Bak S, Beisson F, Bishop G, Hamberger B, Höfer R, Paquette S, Werck-Reichhart D. 2011. Cytochromes p450. *The Arabidopsis Book*. **9**: e0144.

Bednarek P, Osbourn A. 2009. Plant-microbe interactions: chemical diversity in plant defense. *Science* **324**:746-748.

Bednarek P, Pislewska-Bednarek M, Svatos A, Schneider B, Doubsky J, Mansurova M, Humphry M, Consonni C, Panstruga R, Sanchez-Vallet A et al. 2009. A glucosinolate metabolism pathway in living plant cells mediates broad-spectrum antifungal defense. *Science* **323**: 101-106.

Beekwilder J, van Leeuwen W, van Dam NM, Bertossi M, Grandi V, Mizzi L, Soloviev M, Szabados L, Molthoff JW, Schipper B et al. 2008. The impact of the absence of aliphatic glucosinolates on insect herbivory in Arabidopsis. *PLoS One* **3**:e2068.

Bessire M, Chassot C, Jacquat AC, Humphry M, Borel S, Petetot JM, Metraux JP, Nawrath C. 2007. A permeable cuticle in Arabidopsis leads to a strong resistance to *Botrytis cinerea*. *EMBO Journal* **26**: 2158-2168.

Boller T, Felix G. 2009. A renaissance of elicitors: perception of microbe-associated molecular patterns and danger signals by pattern-recognition receptors. *Annual Reviews of Plant Biology* **60**: 379-406.

Dawson GW, Hick AJ, Bennett RN, Donald A, Pickett JA, Wallsgrove RM. 1993. Synthesis of glucosinolate precursors and investigations into the biosynthesis of phenylalkyl- and methylthioalkylglucosinolates. *Journal of Biological Chemistry* **268**: 27154-27159.

de Almeida Engler J, Favery B, Engler G, Abad P. 2005. Loss of susceptibility as an alternative for nematode resistance. *Current Opinion in Biotechnology* **16**:112-117.

Drumm JE, Adams JB, Brown RJ, Campbell CL, Erbes DL, Hall WT, Hartzell SL, Holliday MJ, Kleier DA, Martin MJ et al. 1995. Oxime fungicides – highly active broad-spectrum protectants. In: Baker DR; Fenyes JG; Basarab GS, eds. *Synthesis*

and chemistry of agrochemicals IV. ACS Symposium Series 584, American Chemical Society, Washington, 396-405 .

Fan J, Crooks C, Creissen G, Hill L, Fairhurst S, Doerner P, Lamb C. 2011. *Pseudomonas* sax genes overcome aliphatic isothiocyanate-mediated non-host resistance in *Arabidopsis*. *Science* **331**: 1185-1188.

Green JR, Carver TL, Gurr, SJ. 2002. The formation and function of infection and feeding structures. In: Bélanger RR, Bushnell WR, Dik, AJ, Carver TL, eds. *The Powdery Mildews: A Comprehensive Treatise.* APS Press, St. Paul, Minnesota, 66–82.

Gronover CS, Kasulke D, Tudzynski P, Tudzynski B. 2001. The role of G protein alpha subunits in the infection process of the gray mold fungus *Botrytis cinerea*. *Molecular Plant-Microbe Interactions* **14**: 1293-302.

Hansen CH, Du L, Naur P, Olsen CE, Axelsen KB, Hick AJ, Pickett JA, Halkier BA. 2001. CYP83b1 is the oxime-metabolizing enzyme in the glucosinolate pathway in Arabidopsis. *Journal of Biological Chemistry* **276**: 24790-24796.

Hansjakob A, Riederer M, Hildebrandt U. 2012. Appressorium morphogenesis and cell cycle progression are linked in the grass powdery mildew fungus *Blumeria graminis*. *Fungal Biology* **116**: 890-901.

Hansjakob A, Bischof S, Bringmann G, Riederer M, Hildebrandt U. 2010. Very-long-chain aldehydes promote in vitro prepenetration processes of *Blumeria graminis* in a dose- and chain length-dependent manner. *New Phytologist* **188**: 1039-1054.

Haughn GW, Davin L, Giblin M, Underhill EW. 1991. Biochemical genetics of plant secondary metabolites in *Arabidopsis thaliana*: The glucosinolates. *Plant Physiology* **97**: 217-226.

Hemm MR, Ruegger MO, Chapple C. 2003. The Arabidopsis *ref2* mutant is defective in the gene encoding CYP83A1 and shows both phenylpropanoid and glucosinolate phenotypes. *Plant Cell* **15**:179-194.

Höfer R, Briesen I, Beck M, Pinot F, Schreiber L, Franke R. 2008. The Arabidopsis cytochrome P450 CYP86A1 encodes a fatty acid omega-hydroxylase involved in suberin monomer biosynthesis. *Journal of Experimental Botany* **59**: 2347-2360.

Hückelhoven R, Eichmann R, Weis C, Hoefle C, Proels RK. 2013. Genetic loss of susceptibility: a costly route to disease resistance? *Plant Pathology* **62 (Suppl. 1):** 56–62.

Hückelhoven R. 2005. Powdery mildew susceptibility and biotrophic infection strategies. *FEMS Microbiology Letters* **245**: 9-17.

Hückelhoven R, Panstruga R. 2011. Cell biology of the plant-powdery mildew interaction. *Current Opinion in Plant Biology* **14**: 738-46.

Inada N, Savory EA. 2011. Inhibition of prepenetration processes of the powdery mildew *Golovinomyces orontii* on host inflorescence stems is reduced in the Arabidopsis cuticular mutant *cer3* but not in *cer1*. *Journal of General Plant Pathology* **77**: 273-281.

Ishikawa T, Watanabe N, Nagano M, Kawai-Yamada M, Lam E. 2011. Bax inhibitor-1: a highly conserved endoplasmic reticulum-resident cell death suppressor. *Cell Death and Differentiation* **18**:1271-1278.

Jacobs AK, Lipka V, Burton RA, Panstruga R, Strizhov N, Schulze-Lefert P, Fincher GB. 2003. An Arabidopsis callose synthase, GSL5, is required for wound and papillary callose formation. *Plant Cell* **15**: 2503-2513.

Jacobs S, Zechmann B, Molitor A, Trujillo M, Petutschnig E, Lipka V, Kogel KH, Schäfer P. 2011. Broad-spectrum suppression of innate immunity is required for colonization of Arabidopsis roots by the fungus *Piriformospora indica. Plant Physiology* **156**: 726-740.

Lipka V, Dittgen J, Bednarek P, Bhat R, Wiermer M, Stein M, Landtag J, Brandt W, Rosahl S, Scheel D et al. 2005. Pre- and postinvasion defenses both contribute to nonhost resistance in Arabidopsis. *Science* **310**:1180-1183.

Lolle SJ, Berlyn GP, Engstrom EM, Krolikowski KA, Reiter WD, Pruitt RE. 1997. Developmental regulation of cell interactions in the Arabidopsis fiddlehead-1 mutant: a role for the epidermal cell wall and cuticle. *Developmental Biology* **189**: 311-321.

Maekawa T, Kracher B, Vernaldi S, Ver Loren van Themaat E, Schulze-Lefert P. 2012. Conservation of NLR-triggered immunity across plant lineages. *Proceedings of the National Academy of Sciences, USA* **109**: 20119-20123.

Møller BL. 2010. Plant science. Dynamic metabolons. *Science* **330**: 1328-1329.

Morrissey JP, Osbourn AE. 1999. Fungal resistance to plant antibiotics as a mechanism of pathogenesis. *Microbiology and Molecular Biology Reviews* **63**: 708-724.

Naur P, Petersen BL, Mikkelsen MD, Bak S, Rasmussen H, Olsen CE, Halkier BA. 2003. CYP83A1 and CYP83B1, two nonredundant cytochrome P450 enzymes metabolizing oximes in the biosynthesis of glucosinolates in Arabidopsis. *Plant Physiology* **133**: 63-72.

Nielsen KA, Hrmova M, Nielsen JN, Forslund K, Ebert S, Olsen CE, Fincher GB, Møller BL. 2006. Reconstitution of cyanogenesis in barley (*Hordeum vulgare* L.) and its implications for resistance against the barley powdery mildew fungus. *Planta* **223**: 1010-1023.

Nongbri PL, Johnson JM, Sherameti I, Glawischnig E, Halkier BA, Oelmüller R. 2012. Indole-3-acetaldoxime-derived compounds restrict root colonization in the beneficial interaction between Arabidopsis roots and the endophyte *Piriformospora indica*. *Molecular Plant-Microbe Interactions* **25**: 1186-1197.

Pavan S, Jacobsen E, Visser RG, Bai Y. 2010. Loss of susceptibility as a novel breeding strategy for durable and broad-spectrum resistance. Mol Breed. Jan;25(1):1-12.

Pinot F, Beisson F. 2011. Cytochrome P450 metabolizing fatty acids in plants: characterization and physiological roles. *FEBS Journal* **278**: 195-205.

Podila GK, Rogers L, Kolattukudy PE. 1993. Chemical signals from avocado wax trigger germination and appressorium formation in *Colletotrichum gloeosporioides*. *Plant Physiology* **103**: 267–272.

Reuber TL, Plotnikova JM, Dewdney J, Rogers EE, Wood W, Ausubel FM. 1998. Correlation of defense gene induction defects with powdery mildew susceptibility in *Arabidopsis* enhanced disease susceptibility mutants. *Plant Journal* **16**: 473-485.

Smith CA, Want EJ, O'Maille G, Abagyan R, Siuzdak G. 2006. XCMS: processing mass spectrometry data for metabolite profiling using nonlinear peak alignment, matching, and identification. *Analytical Chemistry* **78**: 779-787.

Sønderby IE, Burow M, Rowe HC, Kliebenstein DJ, Halkier BA. 2010. A complex interplay of three R2R3 MYB transcription factors determines the profile of aliphatic glucosinolates in Arabidopsis. *Plant Physiology* **153**: 348-363.

Sønderby IE, Hansen BG, Bjarnholt N, Ticconi C, Halkier BA, Kliebenstein DJ. 2007. A systems biology approach identifies a R2R3 MYB gene subfamily with distinct and overlapping functions in regulation of aliphatic glucosinolates. *PLoS One* **2**: e1322.

Stotz HU, Sawada Y, Shimada Y, Hirai MY, Sasaki E, Krischke M, Brown PD, Saito K, Kamiya Y. 2011. Role of camalexin, indole glucosinolates, and side chain modification of glucosinolate-derived isothiocyanates in defense of Arabidopsis against *Sclerotinia sclerotiorum*. *Plant Journal* **67**: 81-93.

Sakurada K, Ikegaya H, Ohta H, Fukushima H, Akutsu T, Watanabe K. 2009. Effects of oximes on mitochondrial oxidase activity. *Toxicology Letters* **189**: 110-114.

Thordal-Christensen H. 2003. Fresh insights into processes of nonhost resistance. *Current Opinion in Plant Biology* **6**: 351-357.

Tsuba, M., Katagiri, C., Takeuchi, Y., Takada, Y., Yamaoka, N. 2002. Chemical factors of the leaf surface involved in the morphogenesis of *Blumeria graminis*. *Physiological and Molecular Plant Pathology* **60**: 51-57

Wang Y, Bouwmeester K, van de Mortel JE, Shan W, Govers F. 2013. A novel Arabidopsis-oomycete pathosystem: differential interactions with *Phytophthora capsici* reveal a role for camalexin, indole glucosinolates and salicylic acid in defence. *Plant Cell and Environment* **36**: 1192-1203.

Weis C, Pfeilmeier S, Glawischnig E, Isono E, Pachl F, Hahne H, Kuster B, Eichmann R, Hückelhoven R. 2013. Co-immunoprecipitation-based identification of putative BAX INHIBITOR-1-interacting proteins involved in cell death regulation and plant - powdery mildew interactions. *Molecular Plant Pathology* **14**: 791-802

Wittstock U, Halkier BA. 2002. Glucosinolate research in the Arabidopsis era. *Trends in Plant Science* **7**: 263-270.

Yin R, Messner B, Faus-Kessler T, Hoffmann T, Schwab W, Hajirezaei MR, von Saint Paul V, Heller W, Schäffner AR. 2012. Feedback inhibition of the general phenylpropanoid and flavonol biosynthetic pathways upon a compromised flavonol-3-O-glycosylation. *Journal of Experimental Botany* **63**: 2465-2478.

Zabka V, Stangl M, Bringmann G, Vogg G, Riederer M, Hildebrandt U. 2008. Host surface properties affect prepenetration processes in the barley powdery mildew fungus. *New Phytologist* **177**: 251-263.

Supporting Information

Additional supporting information may be found in the online version of this article.

Figure S1. Basal resistance to *Botrytis cinerea* is reduced in *myb28-1 myb29*-1 and *cyp83a1* mutants.

Figure S2. Comparison of cuticle permeability of *cyp83a1* and *myb28-1 myb29-1* mutants.

Figure S3. Leaf cuticular wax phenotype of *cyp83a1* mutants.

Figure S4. Quantiative analyses of LC-MS metabolite profiles derived from Col-0, *myb28-1 myb29-1*, *cyp83a1-1*, and *cyp83a1-2* extracts.

Figure S5. LC-MS analysis of 5-methylthiopentanaldoxime in *cyp83a1* mutants.

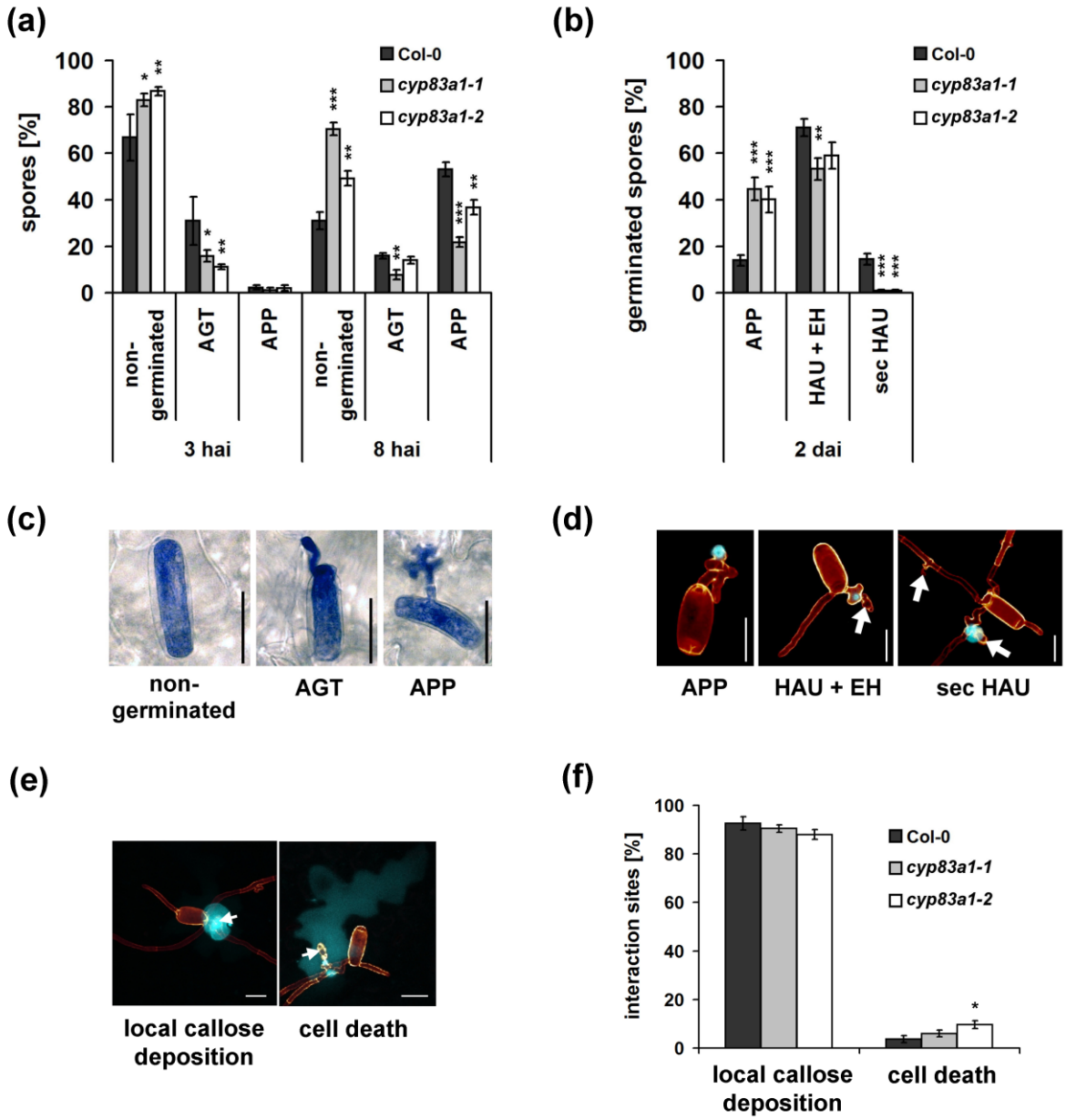

Figure 1. Germination and penetration processes of *E. cruciferarum* are delayed on *cyp83a1* mutants. *Arabidopsis thaliana* Col-0, *cyp83a1-1*, and *cyp83a1-2* plants were inoculated with *E. cruciferarum* and microscopically analyzed regarding the developmental stage of the conidia (a) 3 hai, 8 hai, and (b) 2 dai. The corresponding developmental stages of the fungal structures stained with (c) acetic ink or (d) wheat germ agglutinin-tetramethylrhodamin are depicted. AGT = appressorial germ tube, APP = appressorium, HAU = haustorium (indicated by arrows), EH = elongated hyphae, sec HAU = secondary haustoria. (e) Pictures highlight local or whole cell callose deposition stained by aniline blue as plant

response to fungal attack. Haustoria are marked with arrows. Scale bars = 20 µm. (f) Frequencies of callose depositions at interaction sites. Columns in the graphs represent mean values calculated over a minimum of (a) four leaves with 20 analyzed conidia per time point and genotype or (b, f) ten leaves with 40 germinated conidia per genotype. Bars represent standard errors over the mean values of the single leaves, *, **, and *** represent $P < 0.05$, 0.01, and 0.001, respectively, according to two-sided unpaired Student's t test, calculated over the mean values of single leaves. The experiment was repeated twice with similar results.

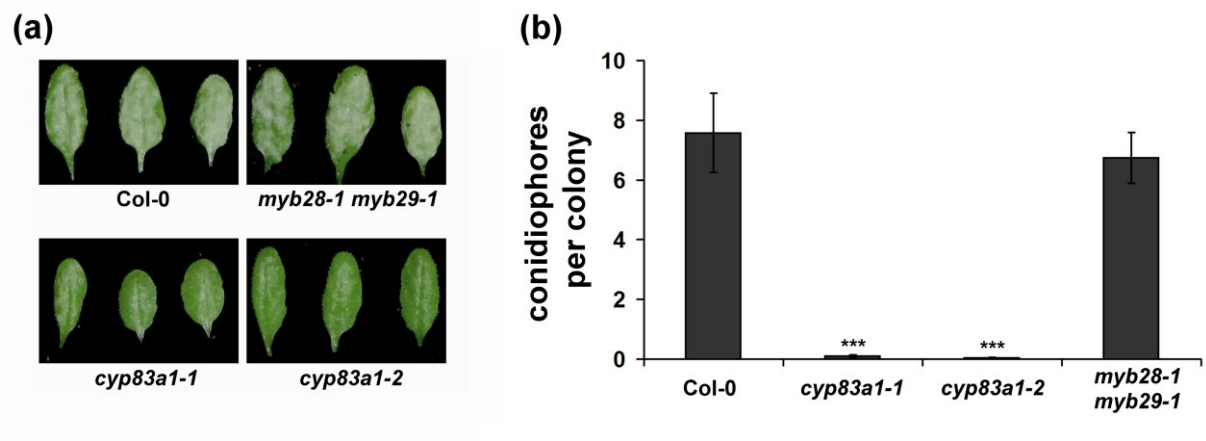

Figure 2. *E. cruciferarum* resistance of *cyp83a1* mutants is independent of a reduced aliphatic glucosinolate level. *Arabidopsis thaliana* Col-0, *cyp83a1-1*, *cyp83a1-2*, and *myb28-1 myb29 -1* plants were inoculated with *E. cruciferarum* conidia. (a) Powdery mildew symptoms photographed 7 dai. (b) Conidiophores per colony were counted 5 dai upon acetic inc staining. 50 colonies per line were evaluated on five individual plants. Columns represent mean values. The experiment was repeated twice with similar results. Bars represent standard errors, *** represent $P < 0.001$, according to two-sided unpaired Student's t test, calculated over the mean values of conidiophores per colony on single leaves.

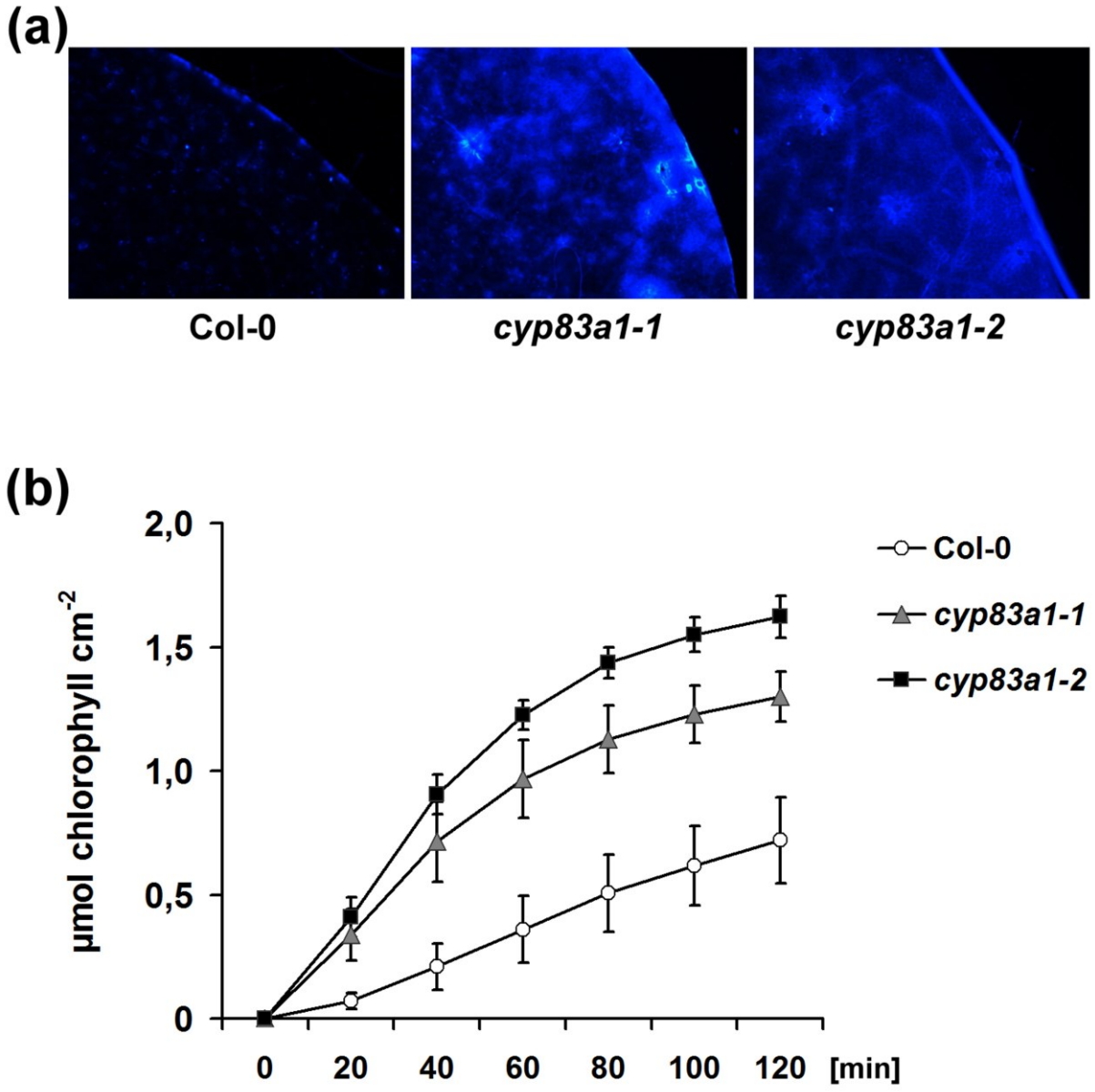

Figure 3. Cuticle permeability phenotype of *cyp83a1* mutants. (a) *Arabidopsis thaliana* Col-0, *cyp83a1-1*, and *cyp83a1-2* leaves were stained with Calcofluor white and imaged under a fluorescence microscope with 5x magnification, using identical settings. The experiment was repeated twice with similar results. (b) Chlorophyll leaching of Col-0, *cyp83a1-1*, and *cyp83a1-2* leaves. Graphs show the amount of chlorophyll per cm^2 leaf surface area extracted as a function of time from leaves immersed in 80% ethanol. The data represent means ± SD of six replicates.

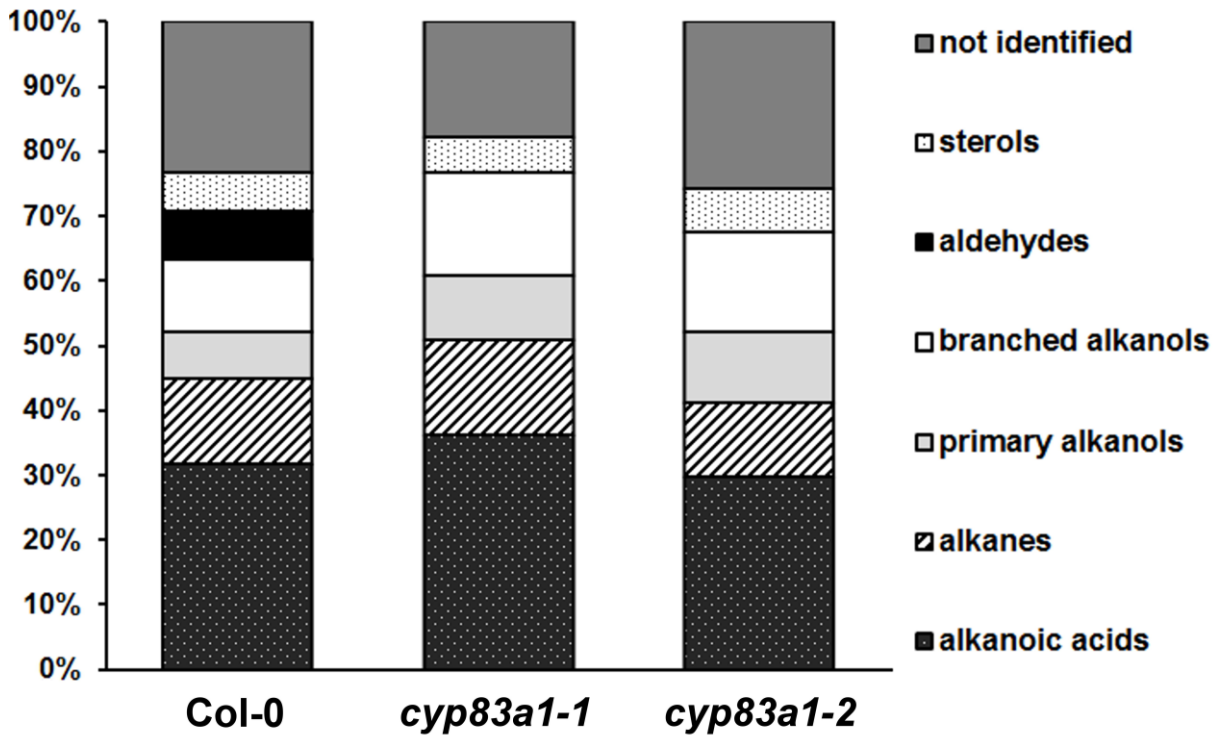

Figure 4. Leaf cuticular wax composition of Col-0 and *cyp83a1* mutants. Percentage of substance classes in the leaf cuticular wax of *Arabidopsis thaliana* Col-0, *cyp83a1-1*, and *cyp83a1-2* are shown as means (n = 5).

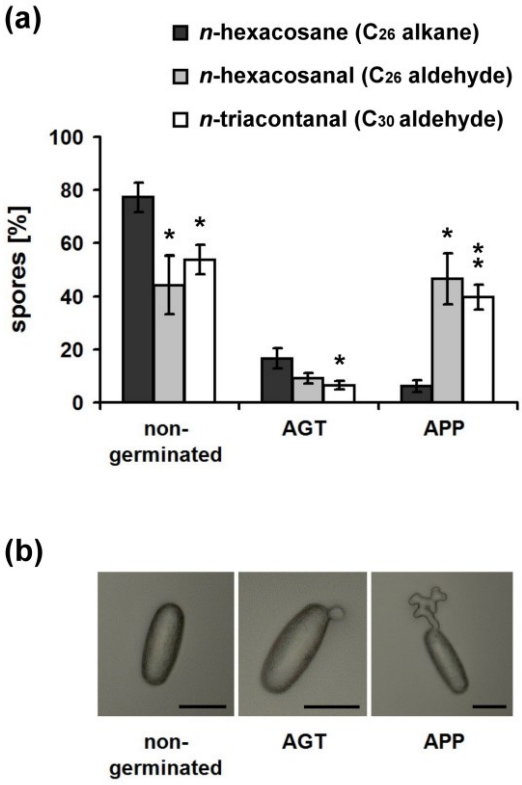

Figure 5. Very-long-chain aldehydes promote germination and differentiation processes of *E. cruciferarum* conidia *in vitro*. (a) Glass slides, coated with Formvar® and the C_{26} alkane *n*-hexacosane, or additionally with the C_{26} aldehyde *n*-hexacosanal or the C_{30} aldehyde *n*-triacontanal, were inoculated with *E. cruciferarum* conidia and microscopically analyzed 9 hai. Developmental stages of the conidia were divided in non-germinated, conidia with an appressorial germ tube (AGT) only, or conidia showing appressorium (APP) formation. Columns represent mean values of at least 5 independent inoculation experiments. In each experiment an average of about 200 conidia were evaluated per variant. Bars represent standard errors, * and ** represent $P < 0.05$ and 0.01, respectively, according to two-sided paired Student's t test. (b) Microscopic pictures show the three different developmental stages of conidia of *E. cruciferarum* analyzed. Scale bar = 20 µm.

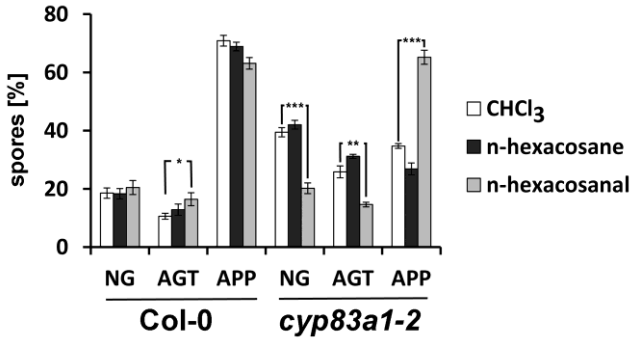

Figure 6. Very-long-chain aldehydes can chemically complement cyp83a1 in terms of differentiation processes of *E. cruciferarum*. Detached leaves of *Arabidopsis thaliana* wild type Col-0 and cyp83a1-2 were sprayed with chloroform as a solvent (mock treatment) of C_{26} alkane *n*-hexacosane solved in chloroform or with the C_{26} aldehyde *n*-hexacosanal solved in chloroform and inoculated with *E. cruciferarum* conidia and microscopically analyzed 8 hai. Developmental stages of the conidia were divided in non-germinated (NG), conidia with an appressorial germ tube (AGT) only, or conidia showing formation of a mature appressorium (APP). Columns represent mean values from 4 individual leaves. Bars represent standard errors, *, ** and *** represent $P < 0.05$, 0.01 and 0.001, respectively, according to two-sided paired Student's t test when $CHCL_3$ control was compared to *n*-hexacosanal treatment.

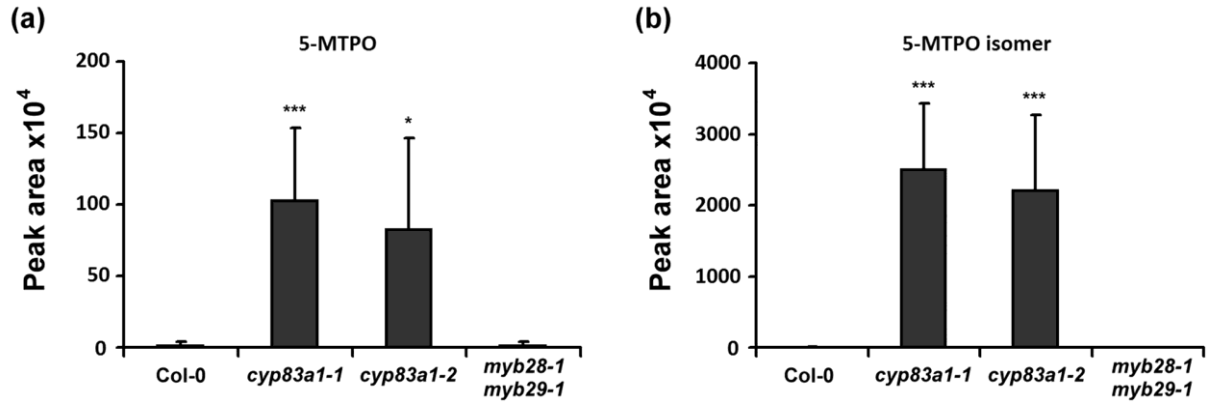

Figure 7. Accumulation of 5-methylthiopentanaldoxime in *cyp83a1* mutants. Methanol-extracts of *Arabidopsis thaliana* Col-0, *cyp83a1-1*, and *cyp83a1-2* were analyzed via analytical LC-MS. 5-methylthiopentanaldoxime (5-MTPO) was used as external standard. 5-MTPO (retention time, 34.1 min) as well as a 5-MTPO isomer (retention time, 27.0 min) was

detected in the ion trace at m z^{-1} 148, respectively. Columns represent means ± SD of six replicates.